ELSEVIER

Journal of Hazardous Materials 68 (1999) 1–17

Journal of Hazardous Materials

www.elsevier.nl/locate/jhazmat

Mineral precipitation and porosity losses in granular iron columns

Patricia D. Mackenzie, David P. Horney, Timothy M. Sivavec *

GE Corporate Research and Development Center, One Research Circle, Niskayuna, NY 12309, USA

Abstract

As permeable reactive barriers containing zero-valent iron are becoming more widely used to remediate contaminated groundwaters, there remains much uncertainty in predicting their long-term performance. This study focuses on two factors affecting performance and lifetime of the granular iron media: plugging at the treatment zone entrance and precipitation in the bulk iron media. Plugging at the system entrance is due principally to mineral precipitation promoted by dissolved oxygen in the influent groundwater and is an issue in aerobic aquifers or in above-ground canister tests. Designs to minimize plugging in field applications where the groundwater is oxygenated include the use of larger iron particles and admixing sand of comparable size with the iron particles. Beyond the entrance zone, the groundwater in anaerobic and mineral precipitation leads to porosity losses in the bulk iron media, potentially reducing flow through the treatment zone. The nature of the mineral precipitation and the factors that affect extent of mineral precipitation have been examined by a variety of tools, including tracer tests, aqueous inorganic profiles, and surface analytical techniques. At short treatment times, porosity losses as measured by tracer tests are due mainly to $Fe(OH)_2$ precipitates and possible entrapment of a film of hydrogen gas on the iron surfaces. Over longer treatment times, precipitation of $Fe(OH)_2$ and $FeCO_3$ in low carbonate waters and of $Fe(OH)_2$, $FeCO_3$ and $CaCO_3$ in higher carbonate waters begin to dominate porosity losses. The control of pH within the iron media by addition of ferrous sulfide was shown not to reduce significantly calcium and carbonate precipitates, indicating that mineral precipitation is controlled by more than simple carbonate equilibrium considerations.

Keywords: Reactive barrier; Groundwater remediation; Corrosion; Iron

* Corresponding author. Tel.: +1-518-387-7677; fax: +1-518-387-5592; e-mail: sivavec@crd.ge.com

0304-3894/99/$ - see front matter
PII: S0304-3894(99)00029-1

1. Introduction

In laboratory columns and in above-ground canister tests, researchers have consistently observed a plugging of the pore spaces at the entrance to the iron system as manifest by the formation of a ''solidified'' zone of iron. Such hardening of the iron particles results in the near 100% occlusion of the pores across a cross section at the entrance to the iron media. In laboratory systems fed with a positive displacement pump, this results in a rapid rise in pressure at the system entrance. In passively-fed systems, the result would be a dramatic reduction in flow through the iron zone.

Previous work in this laboratory suggested that this plugging at the system entrance is due to dissolved oxygen in the influent water [1]. Dissolved oxygen profiles showed that the oxygen is consumed rapidly at the system entrance and does not reach the bulk of the iron media. Dissolved oxygen reacts with the iron at the system entrance to form ferric oxyhydroxides. These amorphous, gelatinous materials can bridge or cement iron particles together, effectively blocking a significant fraction of the pore spaces. Columns run with de-aerated, high carbonate groundwater show no such plugging tendencies. Wavelength dispersive spectroscopy (WDS) of a hardened plug taken from the entrance to an iron column showed no calcium and minimal carbon deposits [2]. These data all point to high dissolved oxygen levels in the groundwater, leading to ferric hydroxide precipitation, as the cause of plugging at the entrance to iron treatment zones.

Because it is associated with high dissolved oxygen levels in the influent water, plugging at the system entrance is anticipated to be an issue only for treatment walls emplaced in aerobic aquifers or in above-ground canister tests where significant dissolved oxygen is introduced by the pumping of water above ground. It is not expected to pose a problem in anaerobic aquifers. Designs that we have proposed to minimize plugging in field applications, where high concentrations of dissolved oxygen in groundwater cannot be avoided, include use of larger iron particles and admixing sand of comparable size with the iron particles [3,4].

Beyond the entrance zone, the groundwater is anaerobic and a second type of mineral precipitation at the iron particle surface has been documented by several research groups [1,5–10]. Mineral precipitation in the bulk media is expected based on groundwater geochemistry and the anaerobic corrosion of zero-valent iron. This mineral precipitation may affect long-term performance of iron walls through effects on system hydraulics (porosity and hydraulic conductivity) and reaction rate. The use of geochemical modeling in predicting precipitate formation in iron barriers has been discussed by Gavaskar et al. [11].

Under the anaerobic conditions that exist in the bulk of the media, iron is reduced by water:

$$Fe^0 + 2H_2O \leftrightarrow Fe^{2+} + H_2(g) + 2OH^- \quad (1)$$

The resultant rise in pH can lead to the precipitation of ferrous hydroxide:

$$Fe^{2+} + 2OH^- \leftrightarrow Fe(OH)_2(s) \quad K_{Fe(OH)2} = 8 \times 10^{-16} \quad (2)$$

In carbonate-containing waters, the rise in pH from the anaerobic corrosion of iron will shift the carbonate–bicarbonate equilibrium and lead to the precipitation of ferrous carbonate (siderite) and calcium carbonate:

$$HCO_3^- + OH^- \leftrightarrow CO_3^{2-} + H_2O \quad pK_a = 10.3 \tag{3}$$

$$Fe^{2+} + CO_3^{2-} \leftrightarrow FeCO_3(s) \quad K_{FeCO_3} = 3.2 \times 10^{-11} \tag{4}$$

$$Ca^{2+} + CO_3^{2-} \leftrightarrow CaCO_3(s) \quad K_{CaCO_3} = 2.8 \times 10^{-9} \tag{5}$$

Thus, three main precipitates may form due to the chemistry in the iron zone: $Fe(OH)_2$, $FeCO_3$, and $CaCO_3$. Each of these precipitates will reduce the pore volume in a granular iron system. Hydrogen produced by the anaerobic corrosion of iron (Eq. (1)) and its retention in the iron media will also lead to porosity losses. Ferrous hydroxide (Eq. (2)) is thermodynamically unstable and may be further oxidized to magnetite according to Eq. (6) at a pH higher than 6–7 [12].

$$3Fe^{2+} + 4H_2O(l) \rightarrow Fe_3O_4(s) + 6H^+ + H_2(g) \tag{6}$$

Under solvent-free simulated groundwater conditions, the formation of ferrous hydroxide and its conversion to magnetite was observed by Odziemkowski et al. using Raman spectroscopy [5].

In this study, we have used several analytical techniques, including tracer tests, aqueous inorganic profiles, and analyses of groundwater-treated granular iron by scanning electron microscopy (SEM), X-ray photoelectron spectroscopy (XPS), and WDS to identify and quantify precipitates that form at the iron surface and to correlate this precipitation with measured system porosity losses.

2. Experimental

2.1. Chemicals

Chlorinated solvents were obtained in high purity and used without further purification. Solvents used included trichloroethylene and *cis*- and *trans*-dichloroethylene (Supelco calibration quality standards) and vinyl chloride (Scott Specialty Gases). Dilute aqueous solutions (typically < 10 mg/l) of one or more of these solvents were prepared by equilibrating neat solvent in 20 l site groundwater for a minimum of 24 h in a well-stirred, glass solution bottle with no headspace and a Teflon cap. The solution was then siphoned under nitrogen positive pressure into a custom-made Teflon PFA collapsible bag ($18 \times 24 \times 24$ in., 0.050 in. film thickness). Groundwater from several sites and with different characteristics were used in this study. In some column experiments, clean site groundwater was sparged with nitrogen to remove dissolved oxygen or was sparged with air to increase the dissolved oxygen concentration prior to introduction to the iron column.

Granular iron was obtained from Peerless Metal Powders and Abrasives (Detroit, MI), Connelly-GPM (Chicago, IL), or VWR Scientific Products. Various mesh sizes of iron were used in column treatability studies. Iron particle sizes ranged from 0.42–1 mm

(−8 + 50 mesh) to 1–4.8 mm (−8 + 16 mesh). Grain size distribution curves are presented in Ref. [3]. Specific surface areas of granular iron, as determined by the BET method using Kr as adsorbate, ranged from 0.98 to 1.75 m^2/g. Cercona pellets (93% iron, balance aluminosilicate; 2.4–3.4 mm, −6 + 8 mesh, P(USMC-1080N)) were obtained from Cercona, Dayton, OH. Granular ferrous sulfide (troilite, as determined by XRD) was obtained from Anachemia, Fisher Scientific and Spectrum Chemical. Specific surface areas of granular FeS ranged from 0.15 to 0.46 m^2/g, as measured by the BET method using Kr as adsorbate.

2.2. Laboratory column methods

Columns were constructed using 2.5 or 5.0 cm diameter thick-walled glass chromatography columns (Ace Glass) of 30 or 60 cm in length, respectively, fitted with Teflon threaded end fittings and sintered glass filter discs (porosity A, Ace Glass). Glass sample ports were added at 2 in. intervals over the entire length of the 5.0 × 60 cm columns and were capped with Teflon-coated septa and crimp-sealed with an aluminum cap. Groundwater from the center axis of the column was sampled using Luer-Lok™ valve-adapted needles inserted into the ports. Columns were also sampled from Teflon PFA Swagelok fittings inserted into the influent and effluent lines. The groundwater solution in the collapsible bag, a Teflon piston pump equipped with a ceramic liner and piston (FMI), the iron column, and a waste container were connected in series with 0.63 in. I.D. and 0.125 in. O.D. Teflon PFA tubing and Teflon PFA Swagelok valve fittings. The 2.5 × 30 cm columns were set in series with sampling between the columns. The direction of water flow was from bottom to top.

Columns were packed by slurring small portions of granular iron in a minimum amount of deionized water and adding them to the columns to ensure that the iron would be homogeneously distributed. All measurements were determined gravimetrically. Typical porosities of 60–65% were achieved when 0.42–1 mm granular iron was used. Groundwater velocities in column studies varied from 0.55 to 46 m/day. Experimental methods for the column tracer tests are reported in Eykholt et al. [13]. All column studies were run at room temperature.

Pressure transducers (Omega, PX-105) were used to monitor pressure increases over the length of iron-packed columns and columns set in series. A dissolved oxygen membrane electrode (Orbisphere or Ingold) and an oxidation reduction potential (ORP) electrode (Ingold Xerolyt® RP-146) were fitted into T-type flow-through cells (In-Flow 724) and were used to monitor continuously column effluents. Velocities for dissolved oxygen and ORP measurements were chosen based on suggestions from Ingold.

Cation analyses, including Ca, Mg, and Fe were determined by inductively coupled plasma atomic emission spectroscopy (ICP/AES). Carbonate measurements were made by ion chromatography.

2.3. Iron analyses

At the conclusion of a column treatability study, iron filings were removed from select regions of the columns, gently washed with acetone, filtered, washed repeatedly

with additional acetone to dry the sample as quickly as possible, then vacuum-dried (<5 mm Hg). This method was shown to minimize the formation of oxides due to oxidation at the iron surface. Dried iron specimens were held under nitrogen gas atmospheres to minimize contamination of surfaces by atmospheric gases. Iron grains were vacuum-impregnated in epoxy and polished to generate cross-sections for analysis by SEM, energy-dispersive X-ray spectroscopy (EDS) and WDS. After curing, the mounts were ground with 180 grit silicon carbide on paper, lapped with 15 μ diamond on a lapping disk, rough polished with 3 μ diamond and 1 μ diamond on a low napped cloth and final-polished with 1 μ diamond on a high napped cloth.

2.4. SEM

Scanning electron micrographs were generated using a Hitachi S-800 field emission secondary electron microscope and a PGT (EDS) Imix/Imagist analyzer. Images were collected with a beam potential of 15 kV.

2.5. EDS and WDS

Iron grains were examined using a Cameca SX50 electron microprobe equipped with a PGT EDS system. Analysis was performed using a 20 keV, 30 nA electron beam. Minerals on the iron surfaces were analyzed using EDS to determine the elements present. Using this technique, X-rays generated from the sample are measured with a Li-drifter Si detector and a spectrum is formed giving a qualitative analysis of the sample in the area under the beam.

Photomicrographs and WDS X-ray dot maps were then taken of oxidized regions of the iron grains. Both secondary electron and backscattered electron images were taken on chosen locations.

2.6. XPS

XPS measurements were made on a Physical Electronics 5500 X-ray photoelectron spectrometer, with a monochromatized Al Kα X-ray source, operated at a power of 400 W. An analyzer pass energy of 187 eV was used for survey scans and 12 eV for high resolution scans of individual core levels. Surface charging was controlled using a low energy electron flood gun (~ 3.0 eV), and the spectra were shifted (after accumulation) to align the C–H component for the C 1s line at 284.6 eV. Atomic concentrations were derived from peak areas using the manufacturer's well-established sensitivity factors. Depth profiles analysis was performed by rasting a 4 kV argon ion beam over an area of 2×2 mm. The ion current was approximately 7 A at an angle of incidence of 45°.

3. Results and discussion

3.1. Plugging at the entrance to iron zones

To establish conclusively that dissolved oxygen in the influent water was the source of the plugging at the entrance to iron systems, a column experiment was conducted in

which a single iron source (0.42–1 mm VWR) was treated with the following waters: site groundwater (300 mg/l carbonate as $CaCO_3$) which had been sparged with nitrogen to remove dissolved oxygen, as-received site groundwater with high dissolved oxygen (4–6 ppm), and deionized water that had been aerated to a high dissolved oxygen concentration (>7 ppm). Fig. 1 summarizes these results. Aerated deionized water rapidly plugged an iron column (2.5×30 cm), as evidenced by the rapid pressure rise (a). In a second column experiment, de-aerated site groundwater showed no plugging tendencies (b), whereas switching to the as-received, highly aerated site groundwater resulted in rapid plugging (c). Note that the negative pressure values are due to a shift in the pressure transducer calibration and do not indicate sub-atmospheric pressures.

When the groundwater was stripped of dissolved oxygen, the column showed no signs of pressure build-up/plugging. When the feed was switched to the as-received groundwater, pressure rose very quickly. In a separate column experiment using aerated deionized water, the pressure rose very quickly from the start. Thus, plugging occurred with water with no carbonate but high dissolved oxygen and did not occur with water with high carbonate and low dissolved oxygen.

Dissolved oxygen profiles were also obtained in column studies purposely run at high groundwater velocities to generate short column residence times. The rapid decline in dissolved oxygen concentration in the groundwater influent is shown in Table 1. These results confirm that dissolved oxygen is the principal source of plugging at column entrances. WDS analysis of a plug taken from the entrance to a plugged iron column showed no calcium, minimal carbon and high levels of iron, confirming that the plugging is due to iron oxides and not due to carbonate precipitates.

Several approaches for scavenging oxygen without leading to system plugging have been identified. Fig. 2 compares two approaches. The rapid pressure rise seen with the smaller iron particles (0.42–1 mm) (a) was dramatically reduced by using larger iron particles (1–4.8 mm) (b), leading to longer system lifetime. The large particles can

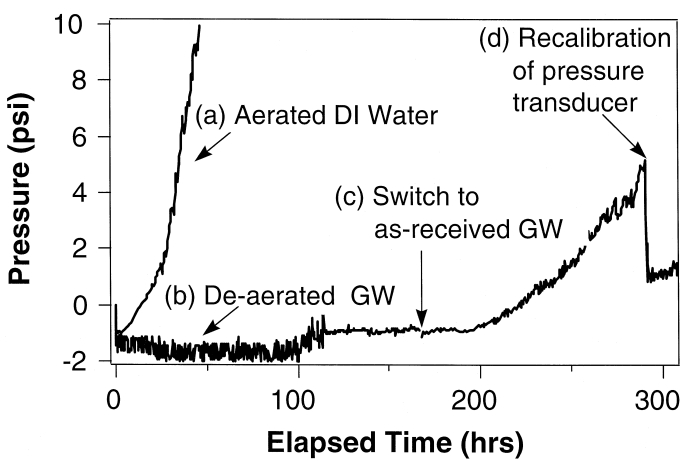

Fig. 1. Iron zone plugging tendencies measured in column treatability tests using waters with different dissolved oxygen concentrations.

Table 1
Dissolved oxygen concentrations measured in 100% granular iron columns set in series. A membrane electrode coupled to a T-type flow-through cell was used to monitor dissolved oxygen in column effluents over 14 days

Cumulative column length (in.)	Column residence time (min)	Dissolved oxygen concentration (ppb)	Standard deviation
0	1.8	5650	70
6	5.4	62	20
18	9.1	49	27
30	12.7	44	29
46	25.7	30	23

afford larger pore spaces and less particle-to-particle contact and therefore are harder to bridge together. Further lifetime extension is achieved by admixing sand particles of the same size with large iron particles (c). In all of these cases, the iron retained its ability to remove dissolved oxygen. Columns packed with Cercona pellets (93% iron, balance aluminosilicate, 2.4–3.4 mm) also indicated no plugging tendencies until they lost their ability to remove dissolved oxygen from the water.

The best system identified to date for scavenging dissolved oxygen from water is one in which large iron particles are admixed with sand of a similar size. Smaller sand particles may become lodged in the pore spaces between iron particles and not serve the role of separating the iron particles and minimizing the particle-to-particle contact that can lead to bridging and plugging. The uniform shape of the Cercona pellets has the same effect.

Our best systems have treated more than 2600 pore volumes of highly aerated water without plugging. For a groundwater flow of 0.3 m/day, this translates to a zone of 0.5 m thick oxygen-scavenging material to yield an operational life of 10 years. Using a less oxygenated water will require a smaller oxygen-scavenging zone. In these designs, it is envisioned that after the oxygen-scavenging zone the bulk media would consist of the

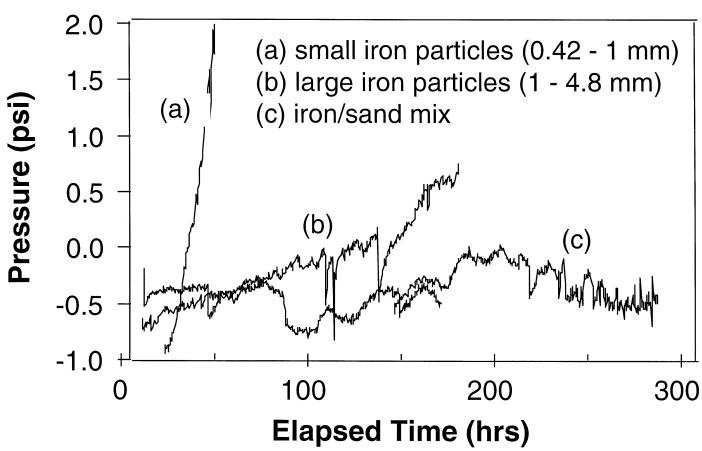

Fig. 2. Approaches to control iron zone plugging due to dissolved oxygen.

more typical iron media (i.e. 100% iron and perhaps smaller particle size) to maximize zone reactivity and minimize zone thickness.

Since plugging is associated with high dissolved oxygen levels, it anticipated to be an issue only for walls emplaced in aerobic aquifers. It is also anticipated to be an issue in ex-situ canister tests where significant dissolved oxygen is introduced by the pumping of water above ground. Plugging should not be an issue in an anoxic aquifer.

4. Porosity changes in the bulk iron media

Mineral precipitation in the bulk iron media can lead to decreases in system porosity and reactivity of iron surfaces. From a variety of techniques, including tracer tests, aqueous inorganic profiles, and surface analysis of iron, it is well established that mineral precipitation and porosity losses occur in iron systems. In order to control precipitation and hence porosity losses, it is important to understand some of the factors that affect mineral precipitation and to understand which precipitates form under given conditions. Factors that affect the type and extent of precipitation include: pH, carbonate level, iron corrosion rate, and residence time in the system. Observations from various treatability studies performed over the last few years will be used to illustrate the impact of these variables [3,10,14]

To measure how porosity changes over time, a tracer test technique suitable for use in iron columns was developed by Eykholt et al. [13]. The technique consists of monitoring the breakthrough curve of a non sorbing tracer (deuterium oxide, D_2O) at various sample ports in a column system. Comparison of measured tracer curves with theoretical predictions, based on the van Genuchten model [15], and with curves measured at the start of the experiment allows estimation of the changes in porosity over time. As discussed above, porosity losses in iron systems can be attributed both to precipitation of three principal minerals, $Fe(OH)_2$, $FeCO_3$ and $CaCO_3$ (Eqs. (2), (4) and (5)) and evolution and retention of hydrogen gas (Eq. (1)). Although no distinct gas bubbles were observed during tracer tests, the formation of a thin film of hydrogen on the surface of the iron particles could be significant in reducing measured porosity.

Fig. 3 shows a set of tracer curves measured at the start and during an iron column experiment [10]. The tracer curves presented are for the second and the third column in an experimental set up consisting of four columns in series. Solid lines denote initial tracer curves and dashed lines denote tracer curves obtained after the columns were treated with a simulated groundwater (40 mg/l $CaCO_3$ with pH adjusted to about 8 with CO_2). At the point when the second tracer test was made, after about 1750 h of operation, 210 pore volumes (2900 l) of simulated groundwater had been introduced to the columns. The measured breakthrough curves correspond to porosity losses of 5–10% throughout the system. A typical inorganic profile measured in a column system is shown in Fig. 4. Most of the loss of inorganics (calcium and carbonate) occur early in these systems. This appears inconsistent with the uniform nature of the porosity losses measured here and in other column studies and suggests that the porosity losses are due either to $Fe(OH)_2$ precipitation or to the formation of a film of hydrogen on the iron particles, processes that would occur throughout the iron zone.

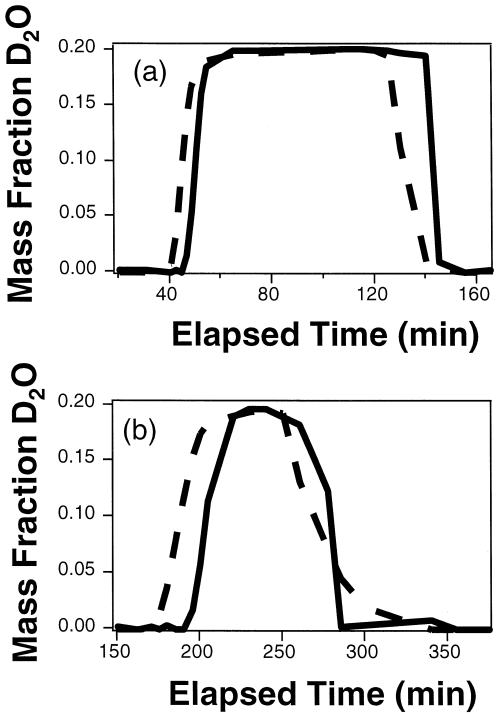

Fig. 3. Porosity losses in the second (a) and third (b) column of a four-column, pilot-scale iron column system were measured by deuterium oxide tracer tests before (solid lines) and after (dashed lines) treatment with low alkalinity, simulated groundwater.

WDS and XPS microscopy are surface analytical methods that have been shown to be useful in determining the speciation of mineral precipitates. Fig. 5 shows the element maps from a WDS scan of iron particles from a column system used to treat over 1500 l of a high carbonate groundwater (approximately 400 mg/l $CaCO_3$). The presence of calcium and carbon indicates the precipitation of calcium carbonate. In contrast, similar scans from iron particles that had been exposed to 2900 l of a low carbonate synthetic groundwater (40 mg/l $CaCO_3$ with pH adjusted to about 8 with CO_2) showed carbon but no calcium, indicating that calcium carbonate precipitation is not significant in low alkalinity waters.

These same precipitation trends are supported by XPS and SEM analysis of cross sections of iron grains. The surfaces of virgin iron grains showed no significant carbonate or calcium concentrations at the passive oxide film surface. Surfaces of iron grains that had been exposed to the low alkalinity/hardness synthetic groundwater in a column showed carbonate but no calcium, indicating the precipitation of $FeCO_3$. After treatment with the high alkalinity/hardness groundwater, the iron particles showed the presence of calcium also, indicating that both $CaCO_3$ and $FeCO_3$ precipitated. Both treated iron particles showed high levels of oxidized iron relative to the virgin material. SEM's of an iron grain removed from this iron column compared to an untreated iron

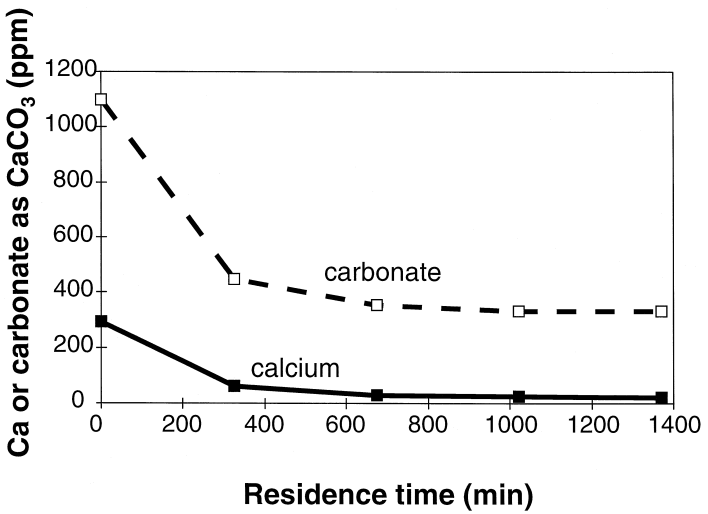

Fig. 4. A typical calcium and carbonate profile measured in an iron column system. The system contained 2880 g of granular iron and had treated 18.5 pore volumes of groundwater at a velocity of 55 cm/day.

grain are displayed in Fig. 6. The relatively low levels of carbonate relative to oxidized iron for these samples suggests that $Fe(OH)_2$ and $FeCO_3$ are present, although caution must be exercised in making such a direct comparison among different iron samples.

Reconciling tracer tests results with this information on mineral precipitation leads to some interesting insights on factors affecting porosity losses. Tracer tests in a variety of studies have consistently shown relatively uniform porosity losses throughout iron column systems, that is, the losses are not associated only with the early zones in a column system where inorganic profiles show the bulk of the calcium and carbonate precipitation occurs.

In addition, mass balances on carbonate losses show only a small portion of the porosity losses measured by tracer tests can be attributed to carbonate precipitates, either calcium or ferrous. For instance, in one study, 2900 l of 40 mg/l calcium carbonate (a total of 1.2 mol) had been introduced into a system at the time a tracer test was performed (Fig. 3). Using a molar volume of 35 ml/mol, representative of $CaCO_3$, this corresponds to about 42 ml of precipitate formed, or about 0.3% of the total system pore volume of 13.6 l. In contrast, the tracer test showed an average 5–10% porosity loss. When a high alkalinity/hardness groundwater was introduced into this system, there was only a small additional decrease in porosity after treating 110 pore volumes of this water.

Given the porous nature of the precipitate formed on iron surfaces as observed by SEM, there is the possibility that the carbonate precipitates effectively occupy a greater volume than their molar volume, essentially trapping stagnant water that is ‘‘lost’’ to the system. Although potentially important, this effect would not result in uniform porosity losses, as most of the inorganic precipitation occurs in the early parts of iron column systems (Fig. 4).

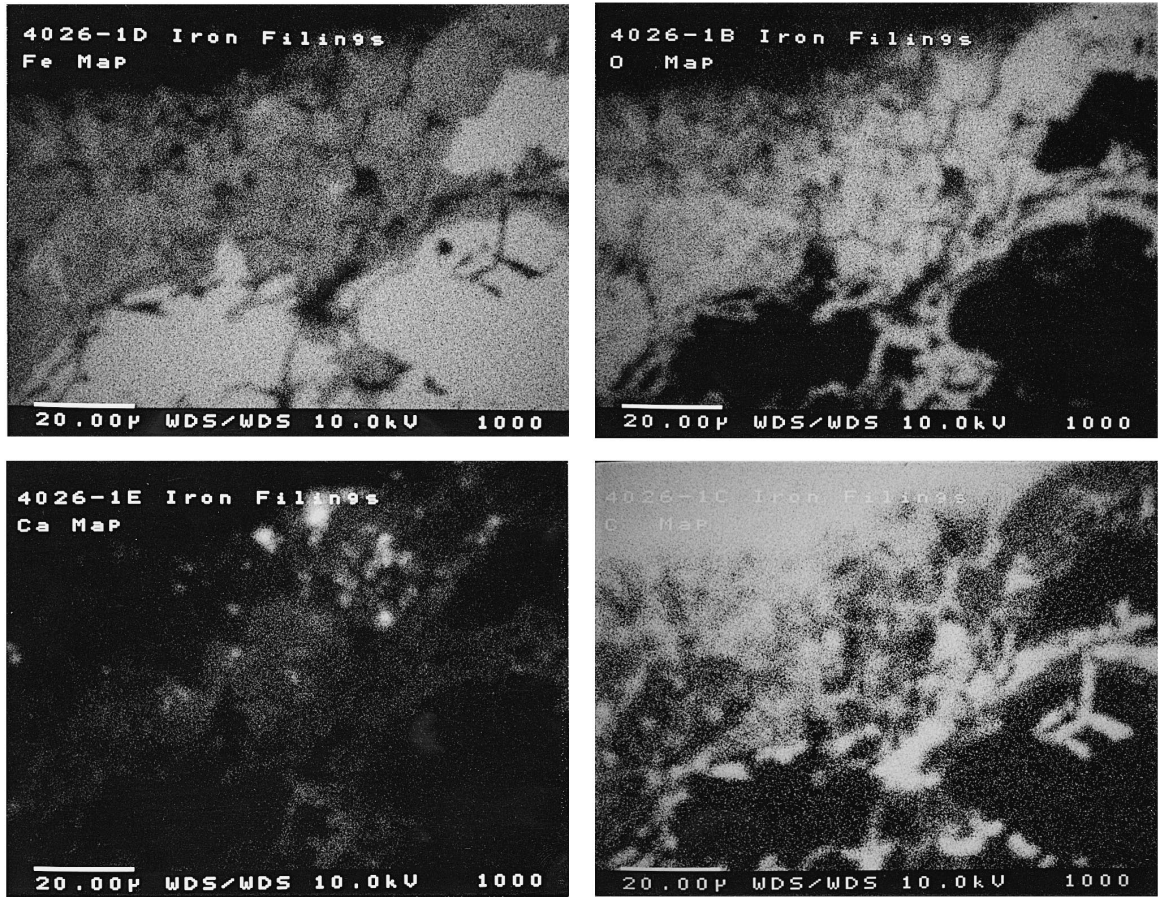

Fig. 5. WDS element maps of a groundwater-treated iron particle. Maps for (a) Fe, (b) O, (c) C, and (d) Ca are shown. Iron particles had been exposed to over 1500 l of a high alkalinity/hardness groundwater in a column treatability study.

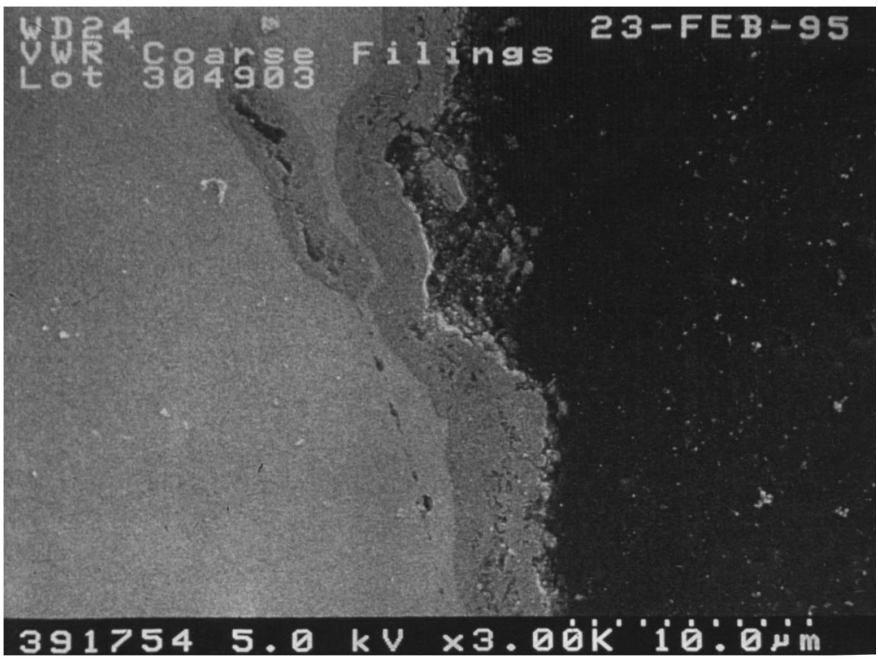
WD24
VWR Coarse Filings
Lot 304903
23-FEB-95
391754 5.0 kV x3.00K 10.0µm

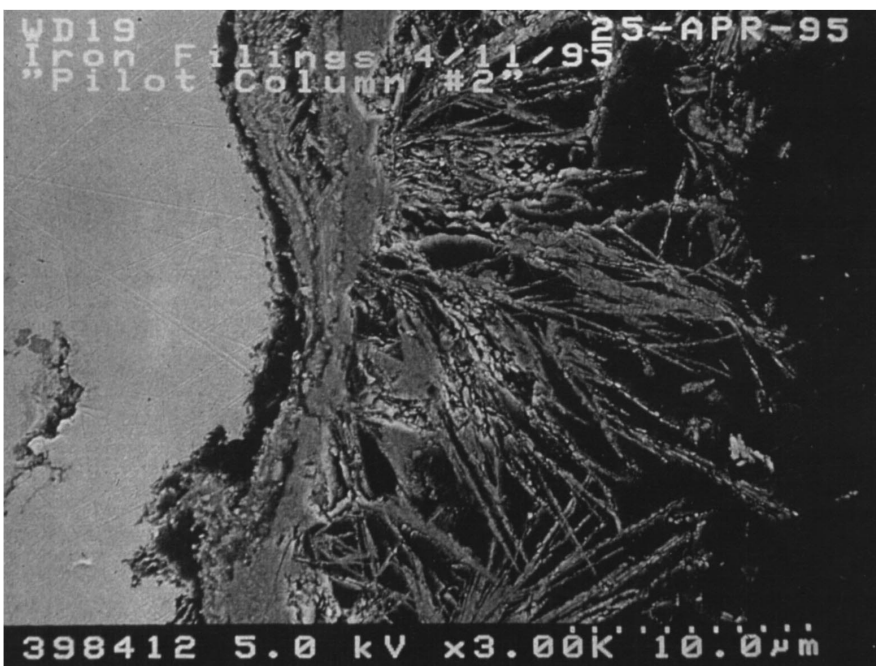
WD19
Iron Filings 4/11/95
"Pilot Column #2"
25-APR-95
398412 5.0 kV x3.00K 10.0µm

Anaerobic corrosion of iron by water would be expected to occur uniformly throughout an iron system. This rate is relatively unaffected by pH in the pH range encountered here [16]. Using measured anaerobic corrosion rates in iron systems of 1 mmol Fe^{2+}/kg iron/day [16], a typical column residence time of 12 h, and a typical iron column loading of about 5 kg iron/l pore water, leads to an Fe^{2+} concentration of 140 ppm. This is far in excess of typical measured total iron levels of 1–10 ppm and, based on the above equilibria, ferrous precipitates are expected to form. Once the bulk of the carbonate precipitation has occurred, the dominant precipitate will be $Fe(OH)_2$. However, using the above corrosion rate, and a molar volume of 26.4 ml/mol for $Fe(OH)_2$, this would still only correspond to about a 1% porosity loss, versus the 5–10% measured by the tracer tests.

This suggests that the porosity losses measured by the tracer tests are not entirely due to mineral precipitation. The production and entrapment of hydrogen may also lead to pore volume reduction. Although gas entrapment in the iron columns in the form of discrete bubbles was not observed, accumulation of a film of H_2 at the iron surface could explain the measured porosity losses. For the system with a pore volume of 13.6 l, the measured 10% porosity loss would require the production of 61 mmol of H_2. At the anaerobic corrosion rates measured by Reardon [16], this amount of H_2 would be produced in about 1 day, although it should be noted that the rates measured by Reardon may be specific to the choice of iron and the conductivity of the water. The leveling off of porosity losses over time suggests that a steady state is reached with respect to H_2 film thickness.

5. Controlling precipitation and porosity losses

Several researchers have found good control of pH in iron systems through the addition of sulfur-based minerals such as pyrite [17] and ferrous sulfide, troilite [18–21]. For instance, Sivavec et al. [19,21] have shown that admixing iron sulfide with granular iron results in controlled pH while still maintaining good reactivity with respect to chloroethene reduction. Modeling results of Holser et al. [17] suggest that a controlled pH will lead to less precipitation. Despite these observations, previous studies have not measured the extent of mineral precipitation and porosity losses in these systems. In addition, it has been suggested that a pH increase within iron media will favor the formation of iron hydroxide $Fe(OH)_2$, which may form a surface layer that inhibits iron dissolution [22,23].

To examine how pH control affects mineral precipitation and porosity losses in iron systems, column studies were undertaken to compare 100% granular iron and 15 wt.% FeS (troilite) and 85 wt.% granular iron as reactive media. Parallel columns were run at

Fig. 6. Scanning electron micrographs of cross-sections of virgin (a) and groundwater-treated iron (b) grains. The treated filing was removed from a column after it had been treated with 215 pore volume of simulated groundwater (40 mg/l $CaCO_3$, pH adjusted to about 8 with CO_2) and 220 pore volumes of site groundwater (approximately 400 mg/l $CaCO_3$).

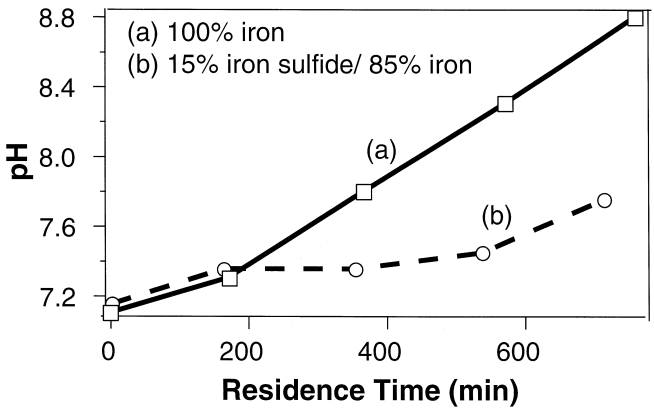

Fig. 7. Profile of pH measured on-line in a 100% granular iron column (a) and a 15% granular ferrous sulfide/85% granular iron column (b). pH control was achieved by the addition of granular ferrous sulfide to the granular iron. Profile was determined after approximately 130 pore volumes of site groundwater was introduced to each 5.0×60 cm column.

a velocity of 1.2 m/day, with about a 12 h residence time over a period in which 165 pore volumes of high alkalinity/hardness site groundwater were introduced. The FeS/Fe system showed good pH control, with the effluent pH about 7.8 versus 8.8 for the Fe-only column (Fig. 7). Inorganic profiles were determined at approximately every 12 pore volumes of groundwater treated. Fig. 8 shows a representative calcium and carbonate concentration profile determined after 165 pore volumes. Despite pH control, the carbonate profiles measured for both the Fe and FeS/Fe columns are quite similar

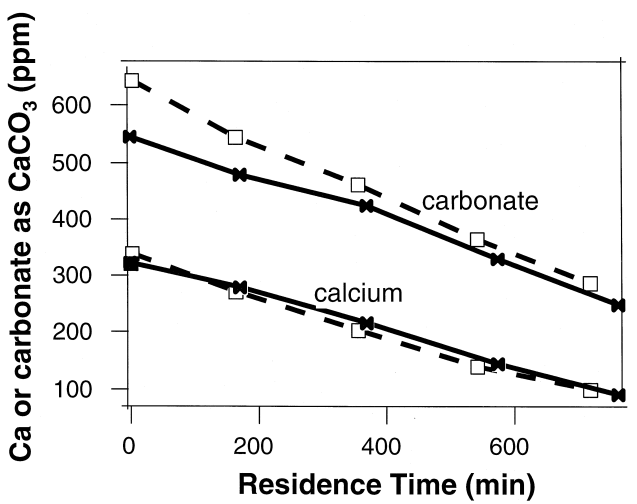

Fig. 8. Calcium and carbonate concentration profiles measured in a 100% granular iron column (solid lines) and a 15% granular ferrous sulfide/85% granular iron column (dashed lines). The profile was determined after approximately 165 pore volumes of site groundwater were introduced to each 5.0×60 cm column. Despite pH control, the loss of calcium and carbonate is remarkably similar throughout the media in both columns.

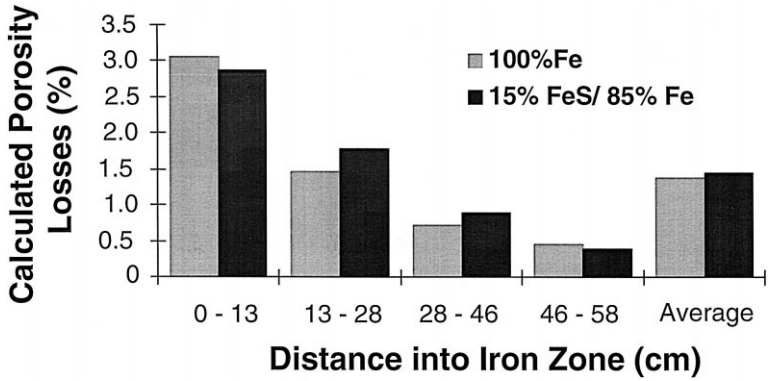

Fig. 9. Porosity losses based on inorganic profiles and molar volume estimates determined for a 100% granular iron column and a 15% granular ferrous sulfide/85% granular iron column. The inorganic profile was measured after approximately 165 pore volumes of site groundwater were introduced to each column.

and the calcium profiles are essentially identical. Equilibrium calculations based on solution pH indicate that calcium and carbonate concentrations would be expected to be an order of magnitude higher at the lower pH. This suggests that solution pH alone does not control the extent of carbonate precipitation and that some other factor(s) must be important. Media porosity losses estimated from the inorganic profiles are shown in Fig. 9. Despite a significantly reduced pH in the FeS/Fe system, calculated porosity losses are very similar in both columns, peaking at about 3.0% early in the media and dropping to about 0.5% late in the media. The two media's reactivity with respect to trichloroethylene remained the same and constant over the entire course of the study. This study has shown that the control of solution pH did not have the expected beneficial effect on calcium and carbonate precipitation and that localized pH at the iron surface may dominate precipitation effects.

6. Conclusions

To date, the effect of mineral precipitation in granular iron treatment zones on system hydraulics (porosity and hydraulic conductivity) and iron reactivity with respect to chlorinated solvent reduction has been found to be small. Plugging at the entrance to an iron treatment zone is due principally to dissolved oxygen in the influent groundwater. Once the dissolved oxygen is removed from the water, groundwater geochemistry and the anaerobic corrosion of the iron (Eq. (1)) control porosity changes within the iron. At short treatment times, porosity losses, as measured by tracer tests, are attributed to $Fe(OH)_2$ precipitates and the likely entrapment of a film of hydrogen gas at the iron surfaces. Over longer treatment times, precipitation of $Fe(OH)_2$ and $FeCO_3$ in low carbonate waters and of $Fe(OH)_2$, $FeCO_3$ and $CaCO_3$ in higher carbonate waters begin to dominate porosity losses. The control of pH (pH range 7.2–7.8) within the iron media by addition of ferrous sulfide did not reduce calcium and carbonate precipitation.

Mineral precipitation appears to be controlled by more than simple carbonate equilibrium considerations based on solution pH.

As cores of granular iron are taken and analyzed from pilot- and full-scale iron treatment walls that have been in place for several years, additional information will be gathered to help develop a model of in situ precipitation rates and other site factors that affect a treatment wall's long-term performance. Encouragingly, field observations acquired over the last year point to porosity losses similar to those observed in our laboratory column treatability studies, which were designed to simulate ''aged'' conditions [24,25].

Acknowledgements

This study was supported in part by the U.S. Department of Energy under contract AC05 840R21400, subcontract 1CP-GEC43C. The authors wish to thank John Chera, Louis Peluso and Lauraine Denault for surface analytical assistance.

References

[1] P.D. Mackenzie, S.S. Baghel, G.R. Eykholt, D.P. Horney, J.J. Salvo, T.M. Sivavec, Pilot-scale demonstration of chlorinated ethene reduction by iron metal: factors affecting iron lifetime, in Emerging Technologies in Hazardous Waste Management VII, Extended Abstracts for the Special Symposium, Atlanta, GA, Industrial and Engineering Chemistry Division, American Chemical Society, 1995, pp. 59–62.

[2] P.D. Mackenzie, T.M. Sivavec, D.P. Horney, Mineral precipitation and porosity losses in iron treatment zones, Prepr. ACS Natl. Meeting, San Francisco, CA 37 (1) (1997) 154–157.

[3] General Electric Corporate Research and Development Center and EnviroMetal Technologies, Treatability Studies: GE Appliances Hazardous Waste UST Closure EPA ID#WID006121347, Final report submitted to Wisconsin Department of Natural Resources, March 1996, pp. 33–42.

[4] P.E. Howson, P.D. Mackenzie, D.P. Horney, Enhanced reactive wall for dehalogenation of hydrocarbons, U.S. Patent 5,543,059, 1996.

[5] M.S. Odziemkowski, T.T. Schuhmacher, R.W. Gillham, E.J. Reardon, Mechanism of oxide film formation on iron in simulating groundwater solutions: raman spectroscopic studies, Corr. Sci. 40 (2–3) (1998) 371–389.

[6] A. Agrawal, P.G. Tratnyek, Reduction of nitro aromatic compounds by zero-valent iron metal, Environ. Sci. Technol. 30 (1996) 153–160.

[7] D.W. Blowes, C.J. Ptacek, J.L. Jambor, In-situ remediation of Cr(VI)-contaminated groundwater using permeable reactive walls: laboratory studies, Environ. Sci. Technol. 31 (1997) 3348–3357.

[8] T.L. Johnson, P.G. Tratnyek, A column study of geochemical factors reductive dechlorination of chlorinated solvents by zero-valent iron, in: G.W. Gee, R.N. Wing (Eds.), In-Situ Remediation: Scientific Basis for Current and Future Technologies, Battelle Press, Richland, WA, 1994, pp. 931–947.

[9] A. Agrawal, P.G. Tratnyek, P. Stoffyn-Egli, L. Liang, Processes affecting nitro reduction by iron metal: mineralogical consequence of precipitation in aqueous carbonate environments, Prepr. Pap. ACS Natl. Meeting, Anaheim, CA 35 (1) (1995) 720–723.

[10] P.D. Mackenzie, S.S. Baghel, G.R. Eykholt, D.P. Horney, J.J. Salvo, T.M. Sivavec, Pilot-scale demonstration of reductive dechlorination of chlorinated ethenes by iron metal, Prepr. Pap. ACS Natl. Meeting, Anaheim, CA 35 (1) (1995) 796–799.

[11] A.R. Gavaskar, N. Gupta, B. Sass, R. Janosy, D. O'Sullivan, Permeable Barriers for Groundwater Remediation: Design, Construction, and Monitoring, Battelle Press, Columbus, OH, 1998.

[12] M. Pourbaix, Lectures on Electrochemical Corrosion, Plenum, New York, 1973, p. 202.
[13] G.R. Eykholt, S.S. Baghel, T.M. Sivavec, P.D. Mackenzie, D.H. Haitko, D.P. Horney, Conservative flow tracers for iron column studies, Prepr. Pap. ACS Natl. Meeting, Anaheim, CA 35 (1) (1995) 818–821.
[14] D.P. Horney, P.D. Mackenzie, J.J. Salvo, T.M. Sivavec, Zero-Valent Iron Treatability Study for Groundwater Contaminated with Chlorinated Organic Solvents at the Paducah, KY GDP Site, Final Report, US DOE Contract No. DE-AC05-840R21400, Subcontract No. 1CP-GEC43C, Dec. 1995.
[15] M.T. van Genuchten, Analytical solutions for chemical transport with simultaneous adsorption, zero-order production and first-order decay, J. Hydrol. 49 (1981) 213–233.
[16] E.J. Reardon, Anaerobic corrosion of granular iron: measurement and interpretation of hydrogen evolution rates, Environ. Sci. Technol. 29 (12) (1995) 2936–2945.
[17] R.A. Holser, S.C. McCutcheon, N.L. Wolfe, Mass transfer effects on the dehalogenation of trichloroethene by iron/pyrite mixtures, Prepr. Pap. ACS Natl. Meeting, Anaheim, CA 35 (1) (1995) 778–779.
[18] T.M. Sivavec, D.P. Horney, Reduction of chlorinated solvents by Fe(II) minerals, Prepr. ACS Natl. Meeting, San Francisco, CA 37 (1) (1997) 115–117.
[19] T.M. Sivavec, D.P. Horney, S.S. Baghel, Reductive dechlorination of chlorinated ethenes by iron metal and iron sulfide minerals, Emerging Technologies in Hazardous Waste Management VII, Extended Abstracts for the Special Symposium, Atlanta, GA, Industrial and Engineering Chemistry Division, American Chemical Society, 1995, pp. 42–45.
[20] T.M. Sivavec, Method for destruction of chlorinated hydrocarbons in aqueous environments, U.S. Patent 5,447,639, 1995.
[21] T.M. Sivavec, D.P. Horney, S.S. Baghel, Method for destruction of halogenated hydrocarbons, U.S. Patent 5,575,927, 1996.
[22] R.W. Gillham, S.F. O'Hannesin, Enhanced degradation of halogenated aliphatics by zero-valent iron, Groundwater 32 (6) (1994) 958–967.
[23] L.J. Matheson, P.G. Tratnyek, Reductive dehalogenation of chlorinated methane by iron metal, Environ. Sci. Technol. 28 (1994) 2045–2053.
[24] J.L. Vogan, B.J. Butler, M.S. Odziemkowski, G. Friday, R.W. Gillham, Inorganic and biological evaluation of cores from permeable iron reactive barriers, Designing and Applying Treatment Technologies: Remediation of Chlorinated and Recalcitrant Compounds, Battelle Press, Columbus, OH, 1998, pp. 163–168.
[25] S.F. O'Hannesin, R.W. Gillham, Long-term performance of an in situ iron wall for remediation of VOCs, Groundwater 36 (1) (1998) 164–170.